JOC Article
pubs.acs.org/joc

Silver(I)−Diene Complexes as Versatile Catalysts for the *C*-Arylation of *N*-Tosylaziridines: Mechanistic Insight from In Situ Diagnostics

Milan Bera[†] and Sujit Roy*[,†,‡]

[†]*Organometallics & Catalysis Laboratory, Chemistry Department, Indian Institute of Technology, Kharagpur 721302, India, and* [‡]*Organometallics & Catalysis Laboratory, School of Basic Sciences, Indian Institute of Technology, Bhubaneswar 751013, India*

royiitkgp@gmail.com; sroychem@iitbbs.ac.in

Received February 27, 2010

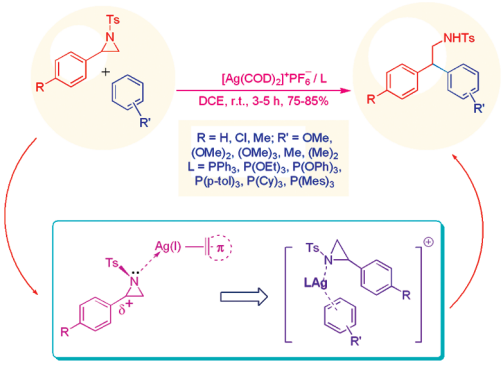

Silver(I) complex $[Ag(diene)_2]^+Y^-$ (where diene = cyclooctadiene, norbornadiene, and 1,3-cyclohexadiene; $Y^- = PF_6^-, BF_4^-$) efficiently catalyzes the arylation of *N*-tosylaziridines with arenes and heteroarenes under ambient condition to provide the corresponding β-aryl amine derivatives with excellent regioselectivity. To understand the nature of substrate activation, and initial bond breaking/making steps, the following studies were conducted with the help of in situ NMR (^1H, ^{31}P, ^{109}Ag) and ESI-MS probe: (I) evaluation of Hammett reaction constant (ρ); (II) correlation of initial rate (k) versus cone angle (θ) of ligand L for reactions mediated by $[Ag(COD)_2]PF_6$/L (where L is a phosphine or a phosphite ligand); (III) identification of silver−arene intermediates in solution; and (IV) correlation of initial rate (k) with $\Delta_{HOMO-LUMO}$ of $[Ag(diene)_2]PF_6$ obtained from preliminary DFT studies. Study I led to a ρ-value of −0.586, indicating that the extent of electrophilic perturbation is considerably less than a typical Lewis acid catalyzed process. Study II indicated that initial rate (k) increases with concomitant increase in θ, as well with $\Delta^{31}P_{(complex-ligand)}$, which corroborates to a mechanism involving prior ligand dissociation. Study III showed the plausible formation of $[Ag(diene)(arene)]^+$ and $[Ag(arene)_2]^+$ as reactive species in solution. Study IV showed that the dependence of initial rate (k) with diene ligand is in the order COD > NBD > CHD; which corresponds well with the order of hardness of the respective Ag(I) complexes.

1. Introduction

Aziridines are important building blocks for the synthesis of various nitrogen-containing organic architectures including natural products and bioactive molecules.[1] A few chosen examples include alkaloids like pumiliotoxin-C, verruculotoxin, and pseudocorhydrin as well as bioactive molecules such as HIV-1 protease inhibitors and tryptophan.[2] Nucleophile-assisted regioselective ring-opening of aziridines has been

(1) (a) Tanner, D. *Angew. Chem., Int. Ed. Engl.* **1994**, *33*, 599. (b) McCoull, W.; Davis, F. A. *Synthesis* **2000**, 1347.

(2) (a) Oppolzer, W.; Flaskamp, E. *Helv. Chim. Acta* **1977**, *60*, 204. (b) Oppolzer, W.; Flaskamp, E.; Bieber, L. W. *Helv. Chim. Acta* **2001**, *84*, 141. (c) Martens, J.; Scheunemann, M. *Tetrahedron Lett.* **1991**, *32*, 1417. (d) Hu, X. E. *Tetrahedron* **2004**, *60*, 2701 and references cited therein. (e) Saha, B.; Nandy, J. P.; Shukla, S.; Siddiqui, I.; Iqbal, J. *J. Org. Chem.* **2002**, *67*, 7858. (f) Nishikawa, T.; Ishikawa, M.; Wada, K.; Isobe, M. *Synlett* **2001**, 945.

Published on Web 06/03/2010 DOI: 10.1021/jo100260k

one of the trustworthy routes to access these architectures.[3] Among the organometallic reagents, those of Li, Cu, and Mg are well-known in promoting facile ring-opening of aziridines.[4] Various silyl nucleophiles such as TMSX (X = Cl, CN, N_3) also effectively react with aziridines in the presence of transition metal catalyst and with organocatalysts.[5] Aziridine carboxylate reacts with carbonyl-stabilized Wittig reagents to provide an isolable phosphorus ylide, and the latter reacts with carbonyl compounds giving rise to optically pure unsaturated amino acids.[6] A variety of Lewis acids such as $Yb(OTf)_3$, $Cu(OTf)_2$, and $Sn(OTf)_2$ and organocatalysts are used in aziridine ring-opening with amine nucleophile to afford the synthetically important diamine compounds.[7] In some cases stoichiometric amount of $MgBr_2$ or ZnX_2 (X = Cl, Br, I) are used as Lewis acid as well as the source for halogen nucleophile for aziridine ring-opening.[8] Alkyl-aryl ethers including amino ethers are important constituents of many pharmacologically active molecules, which can be accessed via the ring-opening of aziridine by *O*-nucleophile.[9] Both arylboronic acid and borate behave as activated nucleophile for aziridine ring-opening. For example, palladium−pincer complex catalyzes the aziridine ring-opening with arylboronic acid, but even without the assistance of a transition metal, aryl borate reacts with aziridine effectively.[10] The cycloaddition of aziridines to dipolarophiles provides a facile entry to heterocycles such as oxazolidine[11] (when carbonyl compound acts as a dipolarophile), imidazoline[12] (when nitrile acts as a dipolarophile), and pyrrolidine[13] (in the case of nonactivated alkenes). The cascade reaction between aziridines and propargylic alcohol containing internal or terminal acetylenic linker affords various *N*,*O*-heterocycles, namely oxazine, oxazepine, and oxazocine.[14] In contrast to the above, there are fewer reports on the regioselective ring-opening of aziridines by an arene nucleophile, which are mostly Lewis acid mediated. To our knowledge the known Lewis acids used include stoichiometric $AlCl_3$ (1 equiv),[15] $BF_3.Et_2O$ (1−3 equiv),[16] catalytic $In(OTf)_3$ (5−10 mol %),[17] $Cu(OTf)_2$ (10 mol %),[18] $AuCl_3$ (5%),[19] and $FeCl_3$ (5%).[20]

Our continuing effort in late transition metal catalysis toward aromatic alkylation reactions[21] prompted us to investigate the reactivity of *N*-tosylaziridines with arene. This endeavor led to the novel finding[22] that under ambient condition, only 1−2% of $AgPF_6$ promotes a highly regioselective ring-opening of *N*-tosylaziridines with a variety of arenes and heteroarenes giving rise to the corresponding β-aryl amine derivatives in excellent yields. Equipped with the above success we next aimed to explore the mechanism of catalysis to better our understanding of the initial bond-breaking and bond-making process and the factors that control these steps. We reasoned that such an exercise would take us to the next logical portal of mechanism-based rational design of ligand to improve the efficiency and selectivity of the catalyst. In the course of these efforts, we found that Ag(I)−diene complexes are equally efficient in promoting the *C*-arylation of aziridines. The Ag(I)−diene complexes are easy to synthesize and purify, have good shelf life, and have turned out to be good candidates for mechanistic studies. In the present article, we delineate the details of the synthetic and mechanistic studies. In the mechanistic front, the following studies were conducted with the help of in situ NMR (^1H, ^{31}P, ^{109}Ag) and ESI-MS probe: (I) evaluation of Hammett reaction constant (ρ) to determine the extent of electrophilic perturbation; (II) correlation of initial rate (k) versus cone angle (θ) of ligand L for reactions mediated by $[Ag(COD)_2]PF_6$/L to understand the ligand influence; and (III) identification of reactive species in solution using ESI-MS and ^{109}Ag NMR as probe to understand Ag−ligand/Ag−arene binding. Aided by preliminary DFT studies we also aimed to correlate the initial rate (k) with $\Delta_{HOMO-LUMO}$ of $[Ag(diene)_2]PF_6$ in order to understand the electronic influence of the diene ligand.

2. Results and Discussion

2.1. Efficacy of $[Ag(COD)_2]PF_6$ as a Catalyst. The initial reaction of *N*-tosyl-2-phenylaziridine **1a** with anisole as the arene as well as the solvent, and $[Ag(COD)_2]PF_6$ (1 mol %) as catalyst at room temperature did not proceed to completion even after 5 h (vide TLC), and workup afforded 50% of *N*-tosyl-2-phenyl-2-(4-methoxyphenyl)ethylamine **2**. In contrast, by using dichloroethane (DCE) as the solvent, the yield of **2** rose to 65% after 5 h (Scheme 1). Gratifyingly, by

(3) (a) Sweeney, J. B. *Chem. Soc. Rev.* **2002**, *31*, 247. (b) Padwa, A.; Murphree, S. S. *ARKIVOC* **2006**, 6. (c) Lu, P. *Tetrahedron*. **2010**, *66*, 2549. (d) Bergmeier, S. C., Lapinsky, D. J. Three Membered Ring Systems. In *Prog. Heterocycl. Chem*. **2009**, *20*, 47; **2009**, *21*, 69.

(4) (a) Kozikowski, A.; Ishida, H.; Isobe, K. *J. Org. Chem*. **1979**, *44*, 2788. (b) Ibuka, T.; Nakai, K.; Habashita, H.; Fujii, N.; Garrido, F.; Mann, A.; Chounan, Y.; Yamamoto, Y. *Tetrahedron Lett*. **1993**, *34*, 7421. (c) Rodrigo, L. O. R. C.; Diego, D. J.; Simonelli, F.; Comasseto, J. V. *Tetrahedron Lett*. **2005**, *46*, 2539.

(5) (a) Wu, J.; Hou, X.-L.; Dai, L.-X. *J. Org. Chem*. **2000**, *65*, 1344. (b) Wu, J.; Sun, X.; Ye, S.; Sun, W. *Tetrahedron Lett*. **2006**, *47*, 4813. (c) Minakata, S.; Okada, Y.; Oderaotoshi, Y.; Komatsu, M. *Org. Lett*. **2005**, *7*, 3509.

(6) Baldwin, J. E.; Adlington, R. M.; Robinson, N. G. *J. Chem. Soc., Chem. Commun*. **1987**, 153.

(7) (a) Meguro, M.; Asao, N.; Yamamoto, Y. *Tetrahedron Lett*. **1994**, *35*, 7395. (b) Sekar, G.; Singh, V. K. *J. Org. Chem*. **1999**, *64*, 2537. (c) Wu, J.; Sun, X.; Li, Y. *Eur. J. Org. Chem*. **2005**, 4271. (d) Cresty, F.; Witt, M.; Frydenvang, K.; Staerk, D.; Jaroszewski, J. W.; Franzik, H. *J. Org. Chem*. **2008**, *73*, 3566.

(8) (a) Righi, G.; Franchini, T.; Bonini, C. *Tetrahedron Lett*. **1998**, *39*, 2385. (b) Ghorai, M. K.; Das, K.; Kumar, A.; Ghosh, K. *Tetrahedron Lett*. **2005**, *46*, 4103. (c) Ghorai, M. K.; Kumar, A.; Tiwari, D. P. *J. Org. Chem*. **2010**, *75*, 137.

(9) (a) Prasad, B. A. B.; Sekar, G.; Singh, V. K. *Tetrahedron Lett*. **2000**, *41*, 4677. (b) Li, P.; Forbeck, E. M.; Evans, C. D.; Joullie, M. M. *Org. Lett*. **2006**, *22*, 5105.

(10) (a) Aydin, J. K. J.; Wallner, O. A.; Saltanova, I. V.; Szabo, J. K. *Chem.—Eur. J*. **2005**, *11*, 5260. (b) Pineschi, M.; Bertolisi, B.; Haak, R. M.; Crotti, P.; Macchia, F. *Chem. Commun*. **2005**, 1426.

(11) (a) Ghorai, M. K.; Ghosh, K. *Tetrahedron Lett*. **2007**, *48*, 3191. (b) Kang, B.; Miller, A. W.; Goyal, S.; Nguyen, S. T. *Chem. Commun*. **2009**, 3928.

(12) Ghorai, M. K.; Ghosh, K.; Das, K. *Tetrahedron Lett*. **2006**, *47*, 5399.

(13) (a) Ungureanu, I.; Koltz, P.; Mann, A. *Angew. Chem., Int. Ed. Engl*. **2000**, *41*, 4615. (b) Loh, T. P.; Hu, Q.-Y.; Ma, L. T. *J. Am. Chem. Soc*. **2001**, *123*, 2450. (c) Dauban, P.; Malik, G. *Angew. Chem., Int. Ed*. **2009**, *48*, 9026.

(14) Bera, M.; Roy, S. *J. Org. Chem*. **2009**, *74*, 8814.

(15) (a) Stamm, H.; Sommer, A.; Woderer, A.; Wiesert, W.; Mall, T.; Assithianakis, P. *J. Org. Chem*. **1985**, *50*, 4946. (b) Stamm, H.; Onistschenko, A.; Buchholz, B.; Mall, T. *J. Org. Chem*. **1989**, *54*, 193.

(16) (a) Bergmeier, S. C.; Kltz, S. J.; Huang, J.; Mcpherson, H.; Donoghue, P. J.; Reed, D. D. *Tetrahedron. Lett*. **2004**, *45*, 5011. (b) Schneider, M. R.; Mann, A.; Taddei, M. *Tetrahedron Lett*. **1996**, *37*, 8493.

(17) Yadav, J. S.; Reddy, B. V. S.; Rao, R. S.; Veerendhar, G.; Nagaiah, K. *Tetrahedron Lett*. **2001**, *42*, 8067.

(18) Hajra, S.; Maji, B.; Mal, D. *Adv. Synth. Catal*. **2009**, *351*, 859.

(19) Sun, X.; Sun, W.; Fan, R.; Wu, J. *Adv. Synth. Catal*. **2007**, *349*, 2151.

(20) Wang, Z.; Sun, X.; Wu, J. *Tetrahedron* **2008**, *64*, 5013.

(21) (a) Choudhury, J.; Podder, S.; Roy, S. *J. Am. Chem. Soc*. **2005**, *127*, 6162. (b) Podder, S.; Choudhury, J.; Roy, S. *J. Org. Chem*. **2007**, *72*, 3129. (c) Podder, S.; Choudhury, J.; Roy, U. K.; Roy, S. *J. Org. Chem*. **2007**, *72*, 3100. (d) Podder, S.; Roy, S. *Tetrahedron*. **2007**, *63*, 9146. (e) Choudhury, J.; Roy, S. *J. Mol. Catal. A: Chem*. **2008**, *279*, 37.

(22) Bera, M.; Roy, S. *Tetrahedron Lett*. **2007**, *48*, 7144.

SCHEME 1. Model Reaction Study

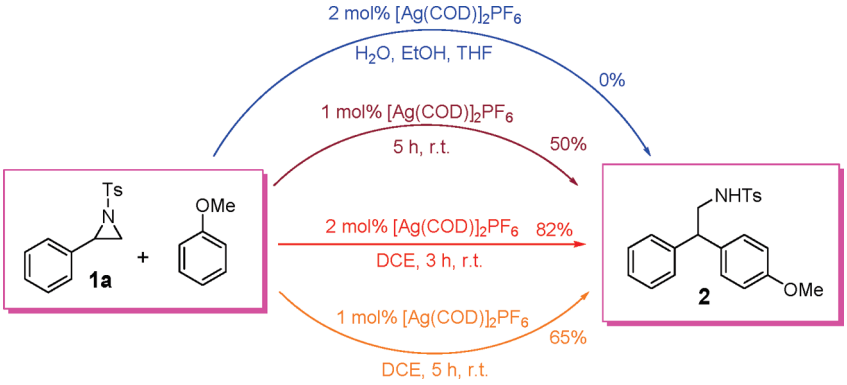

SCHEME 2. C-Arylation of *N*-Tosylaziridine

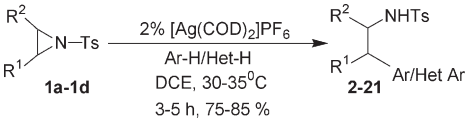

1a: R^1= C_6H_5, R^2= H; **1b**: R^1= 4-ClC_6H_4, R^2= H;
1c: R^1= 4-MeC_6H_4, R^2= H; **1d**: R^1= R^2= C_6H_5

employing 2 mol % of the catalyst, the reaction proceeded to completion within 3 h and amine **2** was isolated in 82% yield. Screening of solvents demonstrated the superiority of DCE over others. Notably the catalytic activity of $[Ag(COD)_2]PF_6$ toward *C*-arylation was inhibited in water, ethanol, and tetrahydrofuran as solvents. Instead, side reactions were predominant. Among the other silver salts and complexes screened for their catalytic activity, only $AgBF_4$ and $[Ag(COD)_2]BF_4$ were promising (Table S1, Supporting Information). The generality of the reaction was successfully tested under the optimized conditions, with *N*-tosylaziridines **1a**−**d** and various arenes and heteroarenes as nucleophiles, giving rise to the corresponding *β*-substituted ethylamines **2**−**21** (Scheme 2, Tables 1 and 2). The products were fully characterized by ^1H, ^{13}C, IR, HRMS, and X-ray crystallography (in case of **6**). The salient remarks are highlighted below.

(1) Arene and heteroarenes always attacked the benzylic position of *N*-tosylaziridines to afford the corresponding product with high regioselectivity.

(2) For ring-activated arenes, reactions were complete within shorter reaction times, and product yields were very good. In contrast, benzene and ring-deactivated arenes were inactive.

(3) The ring-opening reaction was also facilitated with furan and thiophene derivatives, as indicated by shorter reaction time and good yields (Table 2). Clearly, in all cases the substitution took place exclusively at the 2-position of the heteroarene.

(4) The nature of the substituent on the aromatic ring of *N*-tosylaziridine had some effect on the conversion, and the reactivity trend was found to be **1c** > **1a** > **1b** > **1d**.

(5) Attempted arylation with aziridine bearing an alkyl substituent such as *N*-tosyl-2-hexylaziridine and *N*-benzyl-2-phenylaziridine failed.

2.2. Mechanistic Studies. Inspired by the efficacy of the $[Ag(COD)_2]PF_6$ catalysts, and in keeping with our original goal,

TABLE 1. $[Ag(COD)_2]PF_6$-Catalyzed Regioselective Ring-Opening of *N*-Tosylaziridine with Arene as Nucleophile[a]

#	Aziridine	Product	Time(h)	Yield(%)
1		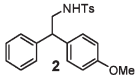	3	82
2	**1a**	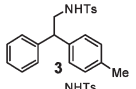	5	75
3	**1a**	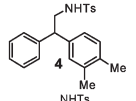	5	79
4	**1a**	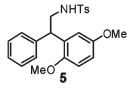	4	85
5	**1a**	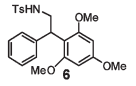	3	88
6	**1a**	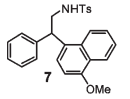	4	80
7	**1a**	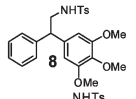	3	85
8	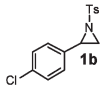	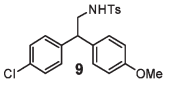	5	80
9	**1b**	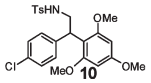	4	84
10	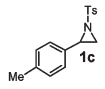	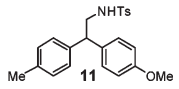	3	85

[a]Conditions: aziridine (1 mmol), arene (2 mmol), $[Ag(COD)_2]PF_6$ (2 mol %), DCE (3 mL).

we next undertook the following mechanistic studies with the help of in situ NMR (^1H, ^{31}P, ^{109}Ag) and ESI-MS probe: (I) evaluation of Hammett reaction constant (ρ) to determine the extent of electrophilic perturbation; (II) correlation of initial rate (k) versus cone angle (θ) of ligand L for reactions mediated by $[Ag(COD)_2]PF_6$/L to understand the ligand influence; (III) identification of reactive species in solution using ESI-MS and ^{109}Ag NMR as probe to understand Ag−ligand/Ag−arene binding; and (IV) correlation of initial rate (k) with $\Delta_{HOMO-LUMO}$ of $[Ag(diene)_2]PF_6$ to understand

TABLE 2. $[Ag(COD)_2]PF_6$-Catalyzed Regioselective Ring-Opening of *N*-Tosylaziridine with Heteroarene as Nucleophile[a]

#	Aziridine	Product	Time(h)	Yield(%)
1	 1a	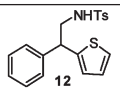 12	3	81
2	1a	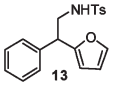 13	4	80
3	1a	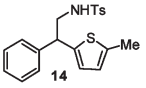 14	3	85
4	1a	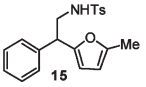 15	4	85
5	1a	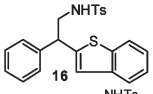 16	4	85
6	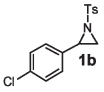 1b	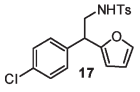 17	4	83
7	1b	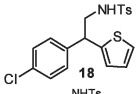 18	4	82
8	1b	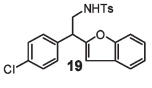 19	4	80
9	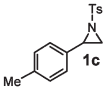 1c	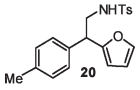 20	3	83
10	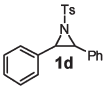 1d	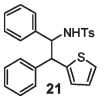 21	5	75

[a]Conditions: aziridine (1 mmol), heteroarene (2 mmol), $[Ag(COD)_2]PF_6$ (2 mol %), DCE (3 mL).

the electronic influence of the diene ligand. The results of these studies are presented below.

Hammett Correlation Study with Substituted Aziridine (Silver−Aziridine Interaction). The effect of substituent on the reaction kinetics is often derived from the Hammett linear free energy relationship [$\log(k_R/k_H) = \rho\sigma$]. From the Hammett plot of relative rate constant values (k_R/k_H) versus the substituent constant (σ), one can obtain the Hammett reaction constant ρ. The latter is a measure of the sensitivity of a reaction to electronic perturbation due to substituent effect. In other words, it is a measure of the relative susceptibility of a reaction to the electron-donating or electron-withdrawing effect exerted by a substituent. We undertook the Hammett study to look into the influence of substituent in aziridine on *C*-arylation. This was attempted by monitoring the product (vide ^1H NMR, with diphenylmethyl toluene as the internal reference) for the initial part of the reaction between anisole and para-substituted phenyl *N*-tosylaziridine in the presence of 1 mol % $[Ag(COD)_2]PF_6$ (Scheme 3, Table 3). The data fitted well with pseudo-first-order rate plots, from which rate constants were evaluated. The linear free energy relationship between the relative rate constant (k_R/k_H) and substituent constant (σ) (Figure 1) resulted in a negative Hammett reaction constant ρ-value (−0.586) indicating an electrophilic mechanism for the present reaction.

SCHEME 3

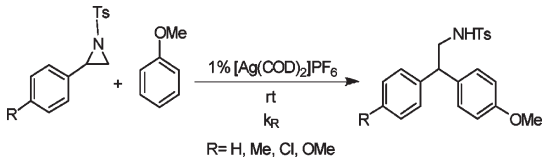

TABLE 3. Rate Constant (k_R) for the Reaction of Anisole with Various Para-Substituted Phenyl *N*- Tosylaziridines

entry	R	σ	$10^4 k_R$ (s^{-1})[a]	k_R/k_H	$\log(k_R/k_H)$
1	OMe	−0.27	2.9	1.380	0.1398
2	Me	−0.17	2.6	1.238	0.0927
3	H	0	2.1	1	0
4	Cl	0.22	1.5	0.714	−0.1463

[a]Error < 5% from 2 runs.

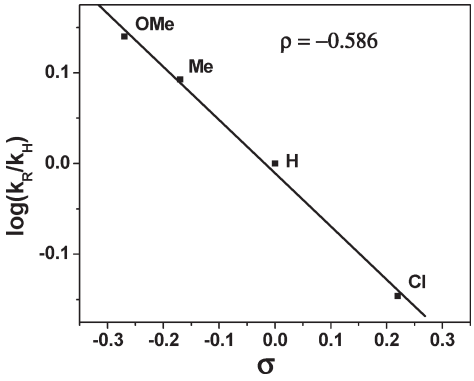

FIGURE 1. $\log(k_R/k_H)$ vs σ of para-substituted phenyl *N*-tosylaziridine.

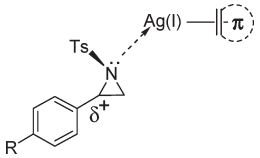

FIGURE 2. Silver−aziridine coordination.

The small negative ρ-value suggests that the catalyst−substrate interaction leads to the generation of a weak positive charge ($\delta+$) at the benzylic ($-CH_2$) carbon center of the aziridine (Figure 2). Absence of a large negative reaction constant ρ-value also indicates that, unlike in the case of strong Lewis acid mediated reactions, in our system "distinct free benzyl cation" is not formed.[23,24]

(23) (a) Sykes, P. *A Guidebook to Mechanism in Organic Chemistry*, 6th ed.; Pearson Education. Inc.: Singapore, 1986. (b) Frost, A. A.; Pearson, R. G. *Kinetics and Mechanism, A Study of Homogeneous Chemical Reactions*; Wiley Interscience: New York, 1961. (c) Laidler, K. J. *Chemical Kinetics*, 3rd ed.; Pearson Education Inc.: Singapore, 1987. (d) March, J. *Advanced Organic Chemistry, Reactions, Mechanisms, and Structure*, 4th ed.; Wiley-Interscience: New York, 1992. (e) Clayden, J.; Greeves, N.; Warren, S.; Wothers, P. In *Organic Chemistry*; Oxford University Press: Oxford, U.K., 2001; pp 1090−1100.

(24) A small Hammett reaction constant ρ-value of −0.586 (within the range from −1 to +1) indicates that the aryl-ring on aziridine is further away from the reactive site. In other words, the δ^+ charge at the site of attack is expected to be less affected by the substituent on the arene ring. To accommodate this view, we prefer the initial binding of aziridine with Ag(I) via the nitrogen center. An alternate binding mode involving Ag(I)−arene π-interaction would markedly alter the ρ-value, hence is less likely. However, a conclusive judgment on this aspect is not possible at this stage. We thank one of the reviewers for raising this issue.

TABLE 4. Changes (Δ, δ, ppm) in the ^{31}P Chemical Shifts[a] of $[Ag(PR_3)_2]PF_6$

ligands (PR_3)	δ (ppm) free ligand	δ (ppm) complex	Δ (ppm)[b]	cone angle (θ) (deg)
$P(OEt)_3$	142.249	125.039	−17.21	109
$P(OPh)_3$	13.432	2.112	−11.32	127
PPh_3	−1.999	17.724	19.723	145
$P(p\text{-tol})_3$	−4.431	19.585	24.086	143
$P(cy)_3$	14.155	46.449	32.294	170
$P(o\text{-tol})_3$	−26.246	−12.576	13.67	194
$P(mes)_3$	−32.998	−26.126	6.872	212

[a]Measurements made in DCE-$CDCl_3$ solvent system, with all the values relative to external H_3PO_4. [b]$\Delta = \delta_{complex} - \delta_{free\ ligand}$.

TABLE 5. Changes (Δ, δ, ppm) in the ^{31}P Chemical Shifts for a Mixture of $[Ag(COD)_2]PF_6$, PR_3, and 2-Phenyl *N*-Tosylaziridine[a]

ligands (PR_3)	δ (ppm) free ligand	δ (ppm) complex	Δ (ppm)	cone angle (θ) (deg)
$P(OEt)_3$	142.495	130.572	−11.923	109
$P(OPh)_3$	12.007	2.301	−9.706	127
PPh_3	−1.757	16.664	18.421	145
$P(p\text{-tol})_3$	−4.183	19.222	23.405	143
$P(cy)_3$	14.411	46.212	31.801	170
$P(o\text{-tol})_3$	−26.237	−13.129	13.108	194
$P(mes)_3$	−32.703	−26.121	6.582	212

[a]Measurements made in DCE-$CDCl_3$ solvent system, with all the values relative to external H_3PO_4.

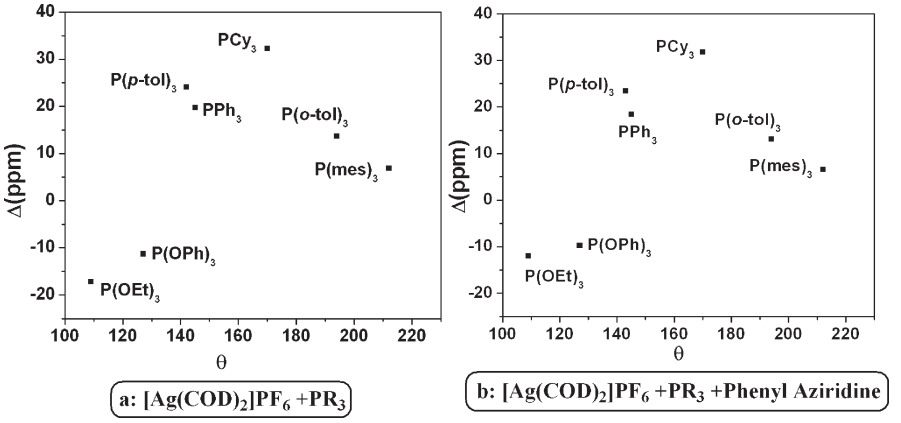

FIGURE 3. Profile of coordination chemical shift (Δ) vs cone angle of phosphorus ligand in $[Ag(COD)_2]PF_6$ catalyst.

SCHEME 4

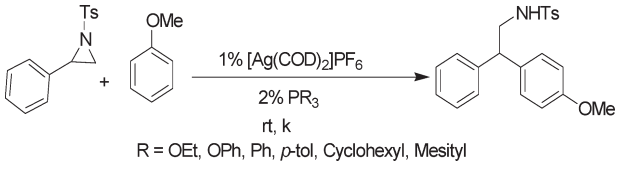

Relating Ligand Cone Angle with ^{31}P NMR Chemical Shift and Initial Rate. Correlating ligand effect with efficiency is an important exercise in the development of a catalyst. In the case of a catalyst bearing phosphine and phosphite ligands it has been found that the steric effect of the ligand influences the catalytic reactivity. Ligand cone angle (also known as Tolman cone angle, and represented by θ) is an important parameter in understanding the steric effect. Ligand cone angle is a measure of the size of a coordinated ligand and is defined as the solid angle (angle in three-dimensional spaces) formed with the metal at the vertex and the hydrogen atoms at the perimeter of the cone. Tertiary phosphine ligands are commonly classified by using this steric parameter. Many studies have established that in metal-mediated coupling reactions, where substrate-binding is an important event, the steric effect of a ligand is equally pertinent as its electronic effect. Therefore, the concept of cone angle is of practical importance in homogeneous catalysis. Indeed, in a number of cases, reaction rates, equilibrium constants, and NMR chemical shifts have been found to correlate well with ligand cone angle.[25]

Keeping the above in view, we desired to confirm whether there is any ligand cone angle dependency on the metal center in the *C*-arylation reaction for Ag(I) catalysts bearing phosphine/phosphites ligands. For this study, we have chosen seven phosphine/phosphite ligands encompassing a cone angle range of 109−212°. The corresponding silver complexes $[Ag(PR_3)_2]PF_6$ were generated in situ by mixing $[Ag(COD)_2]$-PF_6 with 2 equiv of phosphine ligand in a DCE−$CDCl_3$ mixture. In each case ^{31}P NMR spectra were recorded for (i) the free ligand, (ii) the free ligand in the presence of aziridine **1a**, (iii) the in situ generated complex $[Ag(PR_3)_2]PF_6$, and (iv) a mixture of $[Ag(PR_3)_2]PF_6$ and aziridine. From the chemical shift data we determined the coordination chemical shifts $\Delta^{31}P$ which is equal to ($\delta_{complex} - \delta_{free\ ligand}$) (Tables 4 and 5). The corresponding plots of $\Delta^{31}P$ versus θ are shown in Figure 3. In

(25) (a) Tolman, C. A. *Chem. Rev.* **1977**, *77*, 313. (b) Bunten, K. A.; Chen, L.; Fernandez, A. L.; Poe, A. J. *Coord. Chem. Rev.* **2002**, *233*, 41.

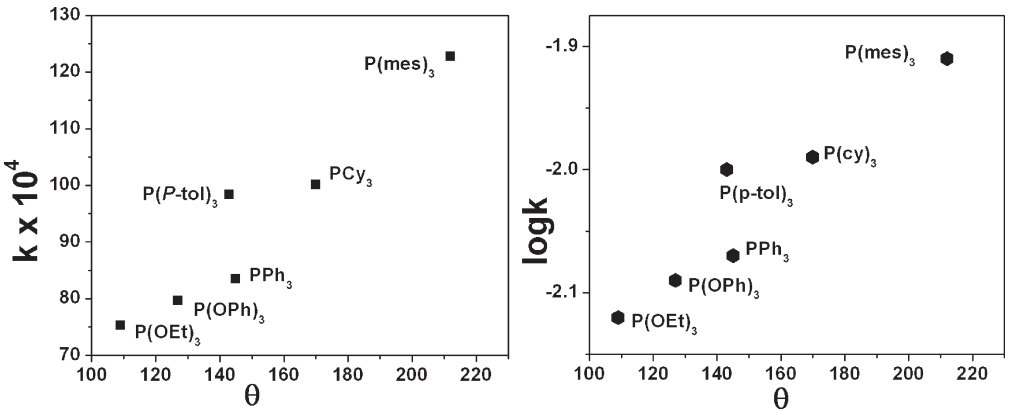

FIGURE 4. Profile of (i) k vs θ and (ii) log k vs θ (θ is the cone angle of phosphorus ligand).

TABLE 6. Rate Constant for the *C*-Arylation of Aziridine with *N*-Tosylphenylaziridine, Anisole, and Different Phosphorus Ligands

ligand	cone angle (deg)	rate constant 10^4k (min^{-1})[a]	log k
$P(OEt)_3$	109	75.3	−2.12
$P(OPh)_3$	127	79.6	−2.09
$P(Ph)_3$	145	83.5	−2.07
$P(p\text{-tol})_3$	143	98.3	−2.00
$P(Cy)_3$	170	100.1	−1.99
$P(mes)_3$	212	122.7	−1.91

[a]Error < 5% from 2 runs.

parallel, the reactivity of the silver(I)−phosphine complexes has been monitored through kinetic study for the reaction of phenyl *N*-tosylaziridine and anisole at 1% catalyst loading (Scheme 4). The rate constant (k) values thus obtained (Table 6) were plotted against cone angle (Figure 4). The pertinent results from the above studies are highlighted below.

(1) For the Ag(I) complexes bearing phosphine ligand, there is a positive coordination chemical shift ($\Delta^{31}P$). Moreover, the shift $\Delta^{31}P$ decreases with increase in cone angle (θ). This is consistent with a steric dependence on NMR—the bulkier ligand being away from the metal center. In contrast, the phosphite ligands show the opposing trend reflecting the dependence on electronic perturbation.[26]

(2) For all the ligands, the rate constants for *C*-arylation (k) increases with simultaneous increase in cone angle of the phosphorus ligand (Figure 4). It is therefore evident that the steric effect of the ligand is dominant in these reactions. We therefore conclude that the mechanism is initiated by prior ligand dissociation.[27]

(3) Since kinetic data indicated that among all the phosphorus ligands $P(mes)_3$ is the most efficient, therefore a bench-scale reaction was attempted with the corresponding Ag(I) complex. The reaction of *N*-tosyl-2-phenylaziridine with anisole in the presence of $[Ag(COD)_2]PF_6$ (2 mol %) and $P(mes)_3$ ligand (4 mol %) afforded **2** in 65% yield after 5 h.

SCHEME 5. Ligand Substitution and Dissociation Steps Involving $[Ag(COD)_2]PF_6$ and PPh_3 in Solution

$$[Ag(COD)_2]^+ \xrightarrow{2\ \text{eqv. } PPh_3} [Ag(PPh_3)_2]^+ \rightleftharpoons [Ag(PPh_3)]^+$$

To gain further evidence of an initial ligand dissociation in the early part of the mechanism, we have subjected a mixture of $[Ag(COD)_2]PF_6$ and PPh_3 (1:2 ratio) in methanol to ESI-MS study under ES(+) mode. The resulting spectrum clearly indicated the formation of species $[Ag(PPh_3)_2]^+$ at m/z 631, $[Ag(PPh_3)(MeOH)]^+$ at m/z 401, and $[Ag(PPh_3)]^+$ at m/z 368.9. This is indicative of (i) the facile replacement of cyclooctadiene by phosphine ligands and (ii) the possibility of $[Ag(PPh_3)]^+$ as a reactive species in solution (Scheme 5).

Diagnosis of Ag(I)−Arene Intermediate in Solution via ESI-MS and ^{109}Ag NMR Probe. Being a d^{10} system Ag(I) is well-known to form π-complexes with olefin, alkyne, and arene.[28] In the case of an olefin, formation of a 1:1 complex $[olefin-Ag]^+$ is predominant; however, complexes such as $[olefin-Ag_2]^{2+}$ and $[(olefin)_2-Ag]^+$ are also known in certain cases. The Ag(I)−olefin bonding follows a η^2-mode and consists of a σ-bond formed by the overlap of a vacant 5s orbital of silver with a filled π-2p orbital of the olefin, and a π-bond formed by the overlap of a filled 4d orbital of the metal with a vacant π^*-2p antibonding orbital of olefin.[29] One may note that the metal olefin bond in $Ag[(COD)_2]PF_6$ (2.50 Å) is longer than that in $Ni(COD)_2$ (2.16 Å), $[Cu(COD)Cl]_2$ (2.05 Å), and $[Pt(COD)_2]$ (2.221 Å).[30−32] As a result olefin−silver(I) complexes are often more labile compared to other d^{10} analogues. Moreover as the double bond character in the silver olefin complexes are less perturbed, therefore ^{1}H NMR or vibrational spectra of the complexes do not differ greatly from those of the free olefins.[33] Keeping the above in view, we attempted mass spectral and ^{109}Ag NMR

(26) (a) Kargol, A. J.; Crecely, R. W.; Burmeister, P. J. *Inorg. Chim. Acta* **1980**, *40*, 79. (b) Miiller, T. E.; Green, J. C.; Mingos, D. N. P.; Mepartlin, C. M.; Whittingham, C.; Williams, D. J.; Woodroffe, T. M. *J. Organomet. Chem.* **1998**, *551*, 313.

(27) (a) Tolman, A. C. *J. Am. Chem. Soc.* **1970**, *92*, 2956. (b) Tolman, A. C. *J. Am. Chem. Soc.* **1970**, *92*, 2953. (c) Moser, R. W.; Marshik-Guerts, J. B.; Okrasinski, J. S. *J. Mol. Catal. A: Chem.* **1999**, *143*, 71. (d) Niyomura, O.; Iwasawa, T.; Sawada, N.; Tokunaga, M.; Obora, Y.; Tsuji, Y. *Organometallics* **2005**, *24*, 3468. (e) Socol, S. M.; Verkade, J. G. *Inorg. Chem.* **1984**, *23*, 3487. (f) Ohta, H.; Tokunaga, M.; Obora, Y.; Iwai, T.; Iwasawa, T.; Fujihara, T.; Tsuji, Y. *Org. Lett.* **2007**, *9*, 89.

(28) Bennett, A. M. *Chem. Rev.* **1961**, 313.

(29) Such synergistic bonding is common in compounds bearing a d-rich metal and a π-ligand. For some historically relevant notes, please see: (a) Winstein, S.; Lucas, H. J. *J. Am. Chem. Soc.* **1938**, *60*, 836. (b) Dewar, M. J. S. *Bull. Soc. Chim. Fr.* **1951**, *18*, C79.

(30) Schunn, R. A.; Ittel, S. D.; Cushing, M. A. *Inorg. Synth.* **1990**, *28*, 94.

(31) Vander, J.; Hende, H.; Baird, W. C. *J. Am. Chem. Soc.* **1963**, *85*, 1003.

(32) Howard, J. A. K. *Acta Crystallogr.* **1982**, *B38*, 2896.

(33) Powell, D. B.; Sheppard, N. *J. Chem. Soc.* **1960**, 2519.

SCHEME 6. Reactive Ag(I)−Arene Species in Reaction Medium

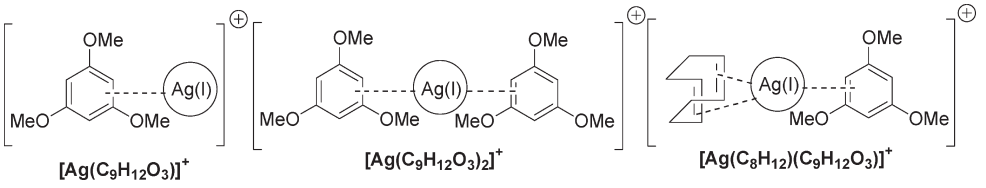

SCHEME 7

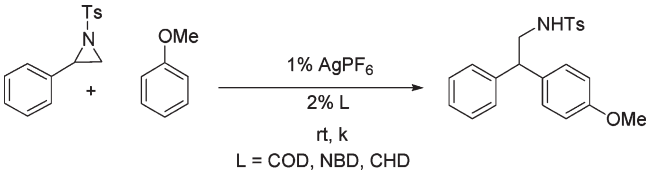

studies to determine the nature of the species present in solution when $AgPF_6$ and $[Ag(COD)_2]PF_6$ interact with arene.

ESI-MS Study. Electrospray ionization mass spectrometry is a soft technique to investigate species in solution. By virtue of having two naturally occurring isotopes (^{107}Ag, ^{109}Ag in 51:49 ratio) silver complexes also allow for easy diagnosis via isotopic mass distribution pattern matching. In the present study trimethoxybenzene ($C_9H_{12}O_3$) was chosen as the representative arene. The studies were conducted with methanolic solutions of $AgPF_6$ or $[Ag(COD)_2]PF_6$ mixed with trimethoxybenzene in 1:2 molar ratio at different cone voltage.

The ES+ mass spectrum (at cone voltage of 30 V) of a solution of $AgPF_6$ and trimethoxybenzene (1:2) is dominated by a peak at m/z 274.8 corresponding to the ion $[Ag(C_9H_{12}O_3)]^+$; there is also a relatively weak peak at m/z 292.8 conforming to the species $[Ag(C_9H_{12}O_3)(H_2O)]^+$. On the contrary, the spectrum recorded at lower cone voltage (15 V) shows a peak at m/z 442.8 corresponding to the ion $[Ag(C_9H_{12}O_3)_2]^+$ beside the peak at m/z 274.8. These results demonstrate that, in the absence of other ligand, the bis-arene complex ion $[Ag(arene)_2]^+$ is labile in solution and dissociates to monoarene complex ion $[Ag(arene)]^+$.

The ES+ mass spectra of $[Ag(COD)_2]PF_6$ and trimethoxybenzene (1:2) at high cone voltage (30 V) show a major peak at m/z 274.8 and a weak peak at m/z 214.9 and are assigned to the species $[Ag(C_9H_{12}O_3)]^+$ and $[Ag(C_8H_{12})]^+$, respectively, whereas the spectrum at low cone voltage (15 V) shows a major peak at 383.1 due to $Ag[(C_8H_{12})(C_9H_{12}O_3)]^+$, and weak peaks at 323.1 and 443.1 assigned to $[Ag(C_8H_{12})_2]^+$ and $Ag[(C_9H_{12}O_3)]_2^+$ respectively.

From the above we conclude that Ag(I)−arene binding remains dominant even in the presence of a diene, with the reactive species in solution being $[Ag(diene)(arene)]^+$ and $[Ag(arene)_2]^+$. It is reasonable to suppose that in solution the Ag(I)−arene species (Scheme 6) could remain in exchange. However, from ESI-MS studies alone, the position of these equilibria cannot be estimated.[34]

^{109}Ag NMR Study. To further look into the Ag(I)−arene binding, we recorded the ^{109}Ag NMR of saturated solutions $AgPF_6$ in $CDCl_3$ before and after the addition of trimethoxybenzene. In the presence of trimethoxybenzene, the ^{109}Ag signal remarkably shifted to 95 ppm.[35] The shift in the Ag NMR indicates that trimethoxybenzene forms a complex with the Ag(I).

TABLE 7. Variation of Reaction Rate (k) with Diene Ligands

no.	diene ligands	10^4k^a (min^{-1})	log k
1	1,5-cyclooctadiene (COD)	127.1	−1.89
2	2,5-norbornadiene (NBD)	115.1	−1.93
3	1,3-cyclohexadiene (CHD)	106.6	−1.97

[a]Error < 5% from 2 runs.

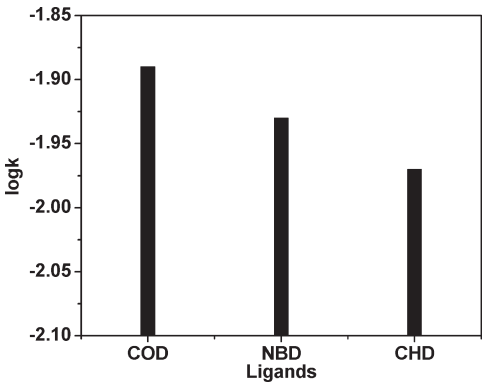

FIGURE 5. Comparison of (log k) for different diene ligands (COD, NBD, CHD).

Effect of Diene Ligand (COD, NBD, 1,3-CHD) on the Efficiency of Ag(I) Catalyst. Since $[Ag(COD)_2]PF_6$ proved to be a good catalyst, we explored the efficacy of other diene ligands on reaction medium. Accordingly, we attempted the kinetic study for the reaction of phenyl *N*-tosylaziridine and anisole in the presence of 1 mol % $AgPF_6$ and 2 mol % diene ligand (Scheme 7). The study was conducted under pseudo-first-order condition and by monitoring the product by ^1H NMR for the initial part of the reaction (with diphenylmethyltoluene as an internal reference). The rate data (Table 7, Figure 5) demonstrate that the catalytic efficiency decreases in the order COD > NBD > CHD.

As in the case of COD, the formation of silver−NBD and CHD complex was confirmed by ESI-MS study, which was carried out by mixing $AgPF_6$ and the diene ligand in 1:2 molar ratio in methanol solvent at different cone voltages. In case of 1,3-cyclohexadiene (CHD) and at high cone voltage

(34) One may recollect that ESI-MS studies only detect the ionic species in a solution. However, there may well be equilibria between ionic and neutral components. Please see: Canty, J. A.; Colton, R. *Inorg. Chim. Acta* **1994**, *220*, 99.

(35) It is noteworthy that among the two NMR active nuclei of silver, namely ^{107}Ag and ^{109}Ag, the latter is more sensitive; hence it is a useful mechanistic tool. The experiment was conducted with saturated solutions of trimethoxybenzene and $AgPF_6$ in $CDCl_3$. The ^{109}Ag spectrum of $AgPF_6$ showed a single peak that was set as zero. Upon addition of trimethoxybenzene to the above, the ^{109}Ag signal shifted to 95 ppm. We could not record the ^{109}Ag NMR spectrum of $[Ag(COD)_2]PF_6$ due to solubility issues. Please see: (a) Goodfellow, R. J., In *Multinuclear NMR*; Mason, J., Ed.; Plenum Press: New York, 1983; pp 563−589. (b) Letinois-Halbes, U.; Pale, P.; Berger, S. J. *J. Org. Chem.* **2005**, *70*, 9185.

SCHEME 8. Catalytic Cycle of *C*-Arylation of *N*-Tosylaziridine

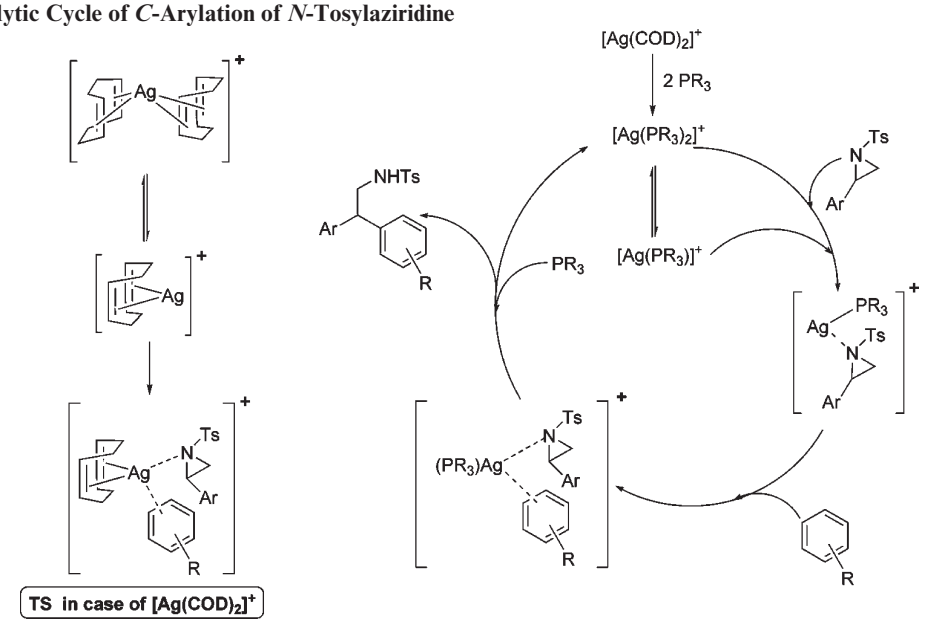

(30 V), the spectrum showed a base peak at m/z 267.3 for $[Ag(CHD)_2]^+$, along with peaks at 187.3 and 219.3 for $[Ag(CHD)]^+$ and $[Ag(CHD)(MeOH)]^+$ species, respectively. But at low cone voltage (15 V) the most dominant peak appeared at 187.3 corresponding to $[Ag(CHD)]^+$ along with a minor peak due to $[Ag(CHD)(MeOH)]^+$. It may be noted that for 2,5-norbornadiene (NBD), the spectrum obtained at both high and low cone voltage were similar, and consisted of a dominant peak at 199.3 for $[Ag(NBD)]^+$ along with a minor peak due to $[Ag(MeOH)(NBD)]^+$ (please see the Supporting Information).

Proposed Catalytic Cycle. By correlating k, σ, θ, and δ, and from the MS and NMR diagnostics, a mechanism is proposed for the present Ag(I) catalyzed arylation reaction (Scheme 8). A few important features of the mechanism are highlighted below.

(1) In the reaction medium phosphine ligand (PR_3) replaces the COD ligand from $[Ag(COD)_2]^+$ species to afford $[Ag(PR_3)_2]^+$. The latter undergoes dissociation to generate the monocoordinated $[Ag(PR_3)]^+$ species.

(2) In reactions where $[Ag(COD)_2]PF_6$ alone is used as the catalyst, $[Ag(COD)]^+$ is the reactive species.

(3) The Ag(I) species having coordinative unsaturation (such as $[Ag(PR_3)]^+$) is capable of further coordination with both aziridine and arene.

(4) The coupling between the two organic partners is facilitated by their close proximity in the Ag-bound activated complex.

DFT Study. To rationalize the observed reactivity pattern of the Ag(I)−diene complexes as discussed above we have performed DFT-calculation to find their HOMO−LUMO energy gap, the latter being a measure of the chemical hardness (η) of the respective complexes. The DFT calculations for the three different Ag(I)−diene complexes were performed with the Gaussian 03 package.[36] The molecular structure and orbital shapes were visualized by using Gaussian view 03 software. The ground state geometries of Ag(I)−diene complexes were optimized by using a PBE1PBE approximation with 6-31G basis set for C and H and sdd basis set for Ag. The geometry of the $Ag(COD)_2^+$ system was taken from experimental X-ray data.

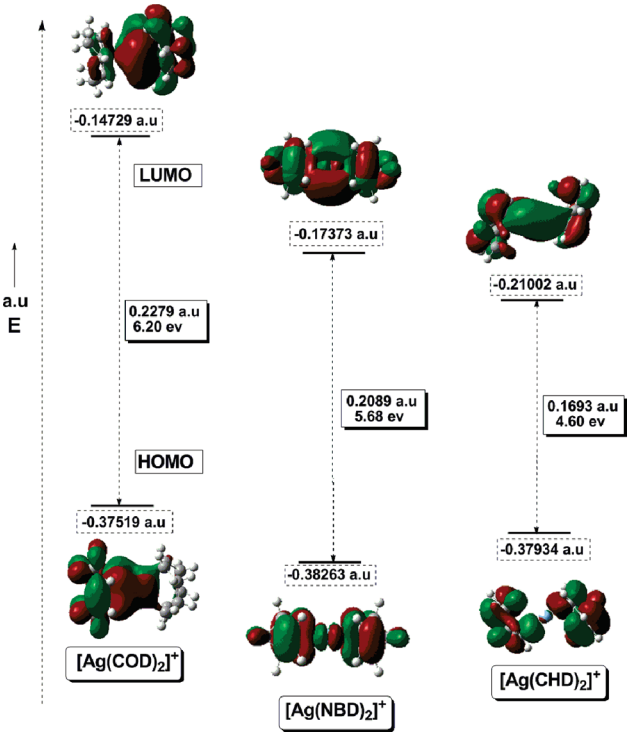

FIGURE 6. Molecular orbital picture of Ag(I)−diene complexes.

The values of chemical hardness (η) depend on HOMO−LUMO energy gap.[37] Hard molecules have a larger HOMO−LUMO gap and soft molecules have a small HOMO−LUMO

(36) Frisch, M. J.; et al. *Gaussion 03*, Revision C.02; Gaussion, Inc.: Wallingford, CT, 2004.

(37) Pearson, G. R. *Acc. Chem. Res.* **1993**, *26*, 250 and references cited therein.

gap. The HOMO−LUMO orbital picture and energy plot of the Ag(I)−diene complexes are shown in Figure 6, from which it is evident that η decreases in the order $[Ag(COD)_2]^+ > [Ag(NBD)_2]^+ > Ag(CHD)_2^+$. Notably the hardness order also reciprocates the order of catalytic efficiency. One may appreciate the relationship, since coordination of both aziridine and arene at the Ag(I) metal center is an important event in the mechanistic cycle.

3. Summary

In summary, we have demonstrated that a number of silver(I) complexes of the type $[Ag(diene)_2]^+Y^-$ (where diene = cyclooctadiene, norbornadiene, and 1,3-cyclohexadiene; $Y^- = PF_6^-$, BF_4^-) act as efficient catalysts for the *C*-arylation of *N*-tosylaziridines with arenes and heteroarenes under ambient condition to provide the corresponding β-aryl amine derivatives with excellent regioselectivity. To understand the nature of substrate activation, and initial bond breaking/making steps, we have performed the following studies with the help of in situ NMR (^1H, ^{31}P, ^{109}Ag) and ESI-MS probe: (I) evaluation of Hammett reaction constant (ρ); (II) correlation of initial rate (k) versus cone angle (θ) of ligand L for reactions mediated by $[Ag(COD)_2]PF_6$/L (where L is a phosphine or phosphite ligand); (III) identification of silver−arene intermediates in solution; and (IV) correlation of the initial rate (k) with $\Delta_{HOMO-LUMO}$ of $[Ag(diene)_2]PF_6$ obtained from preliminary DFT studies. The proposed catalytic cycle invokes a ligand dissociation step as a key step to generate the active catalytic species; the latter then binds both the aziridine and the arene and acts as an anchor for the final coupling stage. The various correlations involving k, σ, θ, and δ values and the results from the MS and NMR studies are in conformity to this proposal. We believe that the mechanistic description presented in this account will aid in future development of catalysts having superior efficiency and selectivity.

4. Experimental Section

General Comments. ^1H NMR spectra were recorded at 400 and 200 MHz. Chemical shifts are reported in ppm from tetramethylsilane with the solvent resonance as the internal standard (chloroform: δ 7.26 ppm). Data are reported as follows: chemical shifts, multiplicity (s = singlet, d = doublet, t = triplet, q = quartet, br = broad, m = multiplet), integration, coupling constant (Hz). ^{13}C NMR spectra were recorded at 100 MHz and 54.6 MHz with proton decoupling. Chemical shifts are reported in ppm from tetramethylsilane with the solvent resonance as the internal standard (chloroform: δ 77.0 ppm). ESI-MS experiments were conducted at +ve ionization mode.

All reactions were carried out under an argon atmosphere in flame-dried glassware, using Schlenk techniques. Chromatographic purifications were done with either 60−120 or 100−200 mesh silica gel. For reaction monitoring, precoated silica gel 60 F_{254} TLC sheets were used. Petroleum ether refers to the fraction boiling in the range 60−80 °C. Dichloroethane was dried and distilled prior to use.

The silver salt of hexafluorophosphate was prepared by a metathetic reaction between equimolar amounts of potassium hexafluorophosphate and silver nitrate in dry acetonitrile medium at room temperature. The reaction completed in just 5 min after which the residue was filtered under argon atmosphere. The filtrate was slowly concentrated under vacuum, when the product separated out as a white salt. It was further recrystallized from acetone/methanol mixture.

General Procedure for the Preparation of *N*-Tosylaziridine (1a−d). To a mixture of styrene (1.16 mL, 10 mmol) and chloramin-T (3.098 g, 11 mmol) in acetonitrile (50 mL) was added phenyltrimethylammonium tribromide (376 mg, 1 mmol) at room temperature. After vigorous stirring for 12 h, the reaction mixture was diluted with ethyl acetate (100 mL) and water (60 mL). The organic layer was separated, washed with brine, and dried over anhydrous Na_2SO_4. After evaporation of the excess solvent, the product was purified by column chromatography on silica gel.

Preparation of $Ag[(COD)_2]PF_6$. To an aqueous solution of $AgPF_6$ (0.5 mmol in 3 mL of water) was added a methanolic solution of 1,5-cyclooctadiene (1 mmol in 0.5 mL of methanol) at room temperature in the absence of light. The reaction completed just after 5 min and the residue was filtered and washed with water and hexane. The white solid was dried under vacuum and was further recrystallized from dichloromethane/benzene solvent system.

Anal. Calcd for $C_{16}H_{26}OAgPF_6$: C, 39.44; H, 5.38. Found: C, 39.46; H, 5.04.

MS (m/z): $Ag[(C_8H_{12})_2]^+$ at 323 at low cone voltage (15 V), $Ag(C_8H_{12})^+$ at 215 at high cone voltage (35 V).

Preparation of $[Ag(COD)_2]BF_4$. To a suspension of $AgBF_4$ (1 g, 5 mmol) in 40 mL of dry dichloromethane under nitrogen at −10 °C was added 12 mL of 1,5-cyclooctadiene through a side arm fitted with a serum cap. After 12 h a white crystalline precipitate was formed. This was filtered off and dried under vacuum. The mother liquor was concentrated under a gentle flow of nitrogen to get a second crop of crystals.

General Procedure for the *C*-Arylation of Tosylaziridine. A mixture of *N*-tosylaziridine (1 mmol), arene or heteroarene (2 mmol), and $[Ag(COD)_2]PF_6$ (2 mol %) in 3 mL of dry dichloroethane was stirred at room temperature. Following completion (vide TLC) the reaction mixture was diluted with water (5 mL) and extracted with dichloromethane. The combined organic layer was dried over anhydrous sodium sulfate then concentrated under vacuum, and the resulting product was purified by column chromatography on silica gel (100−200 mesh, ethyl acetate−petroleum ether, 1:10) to afford pure β-aryl ethylamine derivatives.

Spectral Data of All Compounds. *N*-[2-(4-Methoxyphenyl)-2-phenylethyl]-4-methylbenzenesulfonamide (2): ^1H NMR (400 MHz, $CDCl_3$) δ 2.46 (s, 3H), 3.46−3.57 (m, 2H), 3.78 (s, 3H), 4.02 (t, J = 8 Hz, 1H), 4.29 (t, J = 6 Hz, 1H), 6.82 (d, J = 8.8 Hz, 2H), 7.01 (d, J = 8.4 Hz, 2H), 7.09 (d, J = 6.8 Hz, 2H), 7.20−7.33 (m, 5H), 7.74 (d, J = 8.4 Hz, 2H); ^{13}C NMR (100 MHz, $CDCl_3$) δ 21.6, 47.4, 49.7, 55.3, 114.3, 127.1, 127.2, 127.8, 128.9, 128.9, 129.8, 132.6, 136.7, 141.0, 143.6, 158.6; HRMS (ESI) calcd for $C_{22}H_{23}NO_3S$ $[M + Na]^+$ 404.1296, found 404.1293; IR (KBr) 3283, 2932, 1512, 1324, 1153, 1092, 820 cm^{-1}.

4-Methyl-*N*-(2-phenyl-2-*p*-tolylethyl)benzenesulfonamide (3): ^1H NMR (400 MHz, $CDCl_3$) δ 2.28 (s, 3H), 2.45 (s, 3H), 3.52 (t, J = 7.6 Hz, 2H), 4.00 (d, J = 7.6 Hz, 1H), 4.26 (s, 1H), 6.97 (d, J = 8.0 Hz, 2H), 7.07 (d, J = 7.6 Hz, 2H), 7.20−7.31 (m, 5H), 7.29 (d, J = 8.0 Hz, 2H), 7.69 (d, J = 8.0 Hz, 2H); ^{13}C NMR (100 MHz, $CDCl_3$) δ 20.9, 21.5, 47.2, 50.1, 126.9, 127.1, 127.8, 127.9, 128.8, 129.5, 129.7, 131.1, 136.7, 137.5, 140.8, 143.5; HRMS (ESI) calcd for $C_{22}H_{23}NO_2S$ $[M + H]^+$ 366.1528, found 366.1507; IR (KBr) 3287, 2924, 1598, 1322, 1154, 1093, 816 cm^{-1}.

4-Methyl-*N*-[2-(3,4-dimethylphenyl)-2-phenylethyl]benzenesulfonamide (4): ^1H NMR (400 MHz, $CDCl_3$) δ 2.20 (s, 3H), 2.24 (s, 3H), 2.45 (s, 3H), 3.46−3.55 (m, 2H), 3.98 (t, J = 8 Hz, 1H), 4.28 (br s, 1H), 6.79−6.88 (m, 2H), 7.02−7.09 (m, 3H), 7.18−7.32 (m, 5H), 7.68 (d, J = 8 Hz, 2H); ^{13}C NMR (100 MHz, $CDCl_3$) δ 19.3, 19.8, 21.5, 47.2, 50.0, 125.1, 126.9, 127.1, 128.1, 128.7, 128.7, 129.2, 129.7, 135.4, 136.7, 137.0, 137.9, 138.0, 140.8; DEPT-135 NMR δ

19.3 (CH_3), 19.9 (CH_3), 21.6 (CH_3), 47.3 (CH_2), 50.1 (CH), 125.2 (CH), 126.9 (CH), 127.8 (CH), 128.2 (CH), 128.8 (CH), 129.3 (CH), 129.7 (CH), 130.1 (CH); HRMS (ESI) calcd for $C_{23}H_{25}NO_2S$ $[M + Na]^+$ 402.1504, found 402.1489; IR (KBr) 3281, 2919, 1598, 1327, 1156, 1092, 817 cm^{-1}.

***N*-[2-(2,5-Dimethoxyphenyl)-2-phenylethyl]-4-methylbenzenesulfonamide (5):** ^1H NMR (400 MHz, $CDCl_3$) δ 2.43 (s, 3H), 3.46−3.57 (m, 2H), 3.67 (s, 3H), 3.69 (s, 3H), 4.46 (t, J = 8 Hz, 2H), 6.50 (d, J = 2.8 Hz, 1H), 6.68−6.77 (m, 2H), 7.10 (d, J = 7.2 Hz, 2H), 7.17−7.29 (m, 5H), 7.65 (d, J = 8 Hz, 2H); ^{13}C NMR (100 MHz, $CDCl_3$) δ 21.5, 43.5, 46.2, 55.5, 55.9, 111.5, 111.7, 114.9, 126.8, 127.1, 128.1, 128.6, 129.6, 130.3, 136.7, 140.3, 143.2, 151.2, 153.5; DEPT-135 NMR 21.6 (CH_3), 43.5 (CH), 46.3 (CH_2), 55.6 (CH_3), 56.0 (CH_3), 111.6 (CH), 111.8 (CH), 115.0 (CH), 126.9 (CH), 127.2 (CH), 128.2 (CH), 128.7 (CH), 129.7 (CH); HRMS (ESI) calcd for $C_{23}H_{25}NO_4S$ $[M + Na]^+$ 434.1402, found 434.1386; IR (KBr) 3261, 2928, 2835, 1596, 1329, 1162, 1092, 817 cm^{-1}.

4-Methyl-*N*-[2-phenyl-2-(2,4,6-trimethoxyphenyl)ethyl]benzenesulfonamide (6): ^1H NMR (400 MHz, $CDCl_3$) δ 2.42 (s, 3H), 3.61 (s, 6H), 3.66−3.76 (m, 2H), 3.79 (s, 3H), 4.38 (br s, 1H), 4.65 (t, J = 7.2 Hz, 1H), 6.05 (s, 2H), 7.09−7.20 (m, 5H), 7.25 (d, J = 6.5 Hz, 2H), 7.66 (d, J = 8 Hz, 2H); ^{13}C NMR (100 MHz, $CDCl_3$) δ 21.4, 39.6, 45.2, 55.2, 55.4, 91.0, 108.8, 125.9, 127.1, 127.7, 127.9, 129.4, 137.0, 141.8, 142.8, 159.2, 160.3; HRMS (ESI) calcd for $C_{24}H_{27}NO_5S$ $[M + Na]^+$ 464.1508, found 464.1499; IR (KBr) 3289, 2939, 2839, 1610, 1325, 1164, 1094, 809 cm^{-1}.

***N*-[2-(4-Methoxynaphthyl)-2-phenylethyl]-4-methylbenzenesulfonamide (7):** ^1H NMR (200 MHz, $CDCl_3$) δ 2.42 (s, 3H), 3.64−3.66 (d, J = 3.6 Hz, 2H), 3.98 (s, 3H), 4.61 (br s, 1H), 4.71−4.79 (t, J = 8 Hz, 1H), 6.71−6.75 (d, J = 8 Hz, 1H), 7.11−7.30 (m, 7H), 7.35−7.45 (m, 3H), 7.56−7.61 (d, J = 8.4 Hz, 2H), 7.68−7.77 (m, 1H), 8.26−8.30 (m, 1H); ^{13}C NMR (54.6 MHz, $CDCl_3$) δ 21.6, 45.7, 47.2, 55.5, 103.0, 122.8, 123.1, 124.4, 125.1, 126.3, 126.9, 127.0, 127.2, 128.1, 128.1, 128.9, 129.8, 132.6, 136.9, 141.2, 143.4, 154.9; HRMS (ESI) calcd for $C_{26}H_{25}NO_3S$ $[M + Na]^+$ 454.1453, found 454.1452.

***N*-[2-(3,4,5-Trymethoxyphenyl)-2-phenylethyl]-4-methylbenzenesulfonamide (8):** ^1H NMR (200 MHz, $CDCl_3$) δ 2.43 (s, 3H), 3.47 (d, J = 8 Hz, 2H), 3.60 (s, 3H), 3.81 (s, 6H), 4.33 (t, J = 8 Hz, 1H), 6.54 (d, J = 8.6 Hz, 1H), 6.68 (d, J = 8.6 Hz, 1H), 7.07 (d, J = 9.4 Hz, 2H), 7.13−7.30 (m, 5H), 7.65 (d, J = 8.2 Hz, 2H); ^{13}C NMR (54.6 MHz, $CDCl_3$) δ 21.5, 43.7, 46.7, 55.9, 60.7, 107.3, 122.0, 126.8, 127.2, 128.0, 128.7, 129.7, 136.9, 141.3, 142.5, 143.4, 151.9, 152.8; DEPT-135 NMR δ 21.5 (CH_3), 43.7 (CH), 46.7 (CH_2), 55.9 (OCH_3), 60.7 (OCH_3), 107.3 (CH), 122.0 (CH), 126.8 (CH), 127.1 (CH), 128.0 (CH), 128.7 (CH), 129.7 (CH); HRMS (ESI) calcd for $C_{24}H_{27}NO_5S$ $[M + H]^+$ 442.1683, found 442.1684.

***N*-[2-(4-Chlorophenyl)-2-(4-methoxyphenyl)ethyl]-4-methylbenzenesulfonamide (9):** ^1H NMR (400 MHz, $CDCl_3$) δ 2.44 (s, 3H), 3.45−3.51 (m, 2H), 3.77 (s, 3H), 4.00 (t, J = 8 Hz, 1H), 4.26 (t, J = 6 Hz, 1H), 6.81 (d, J = 8.4 Hz, 2H), 6.96−7.04 (m, 4H), 7.19−7.31 (m, 6H), 7.67 (d, J = 8.4 Hz, 2H); ^{13}C NMR (100 MHz, $CDCl_3$) δ 21.5, 47.2, 49.1, 55.3, 114.3, 127.0, 129.1, 129.4, 129.6, 129.7, 132.0, 132.6, 136.6, 139.6, 143.5, 158.7; DEPT-135 NMR δ 21.6 (CH_3), 47.3 (CH_2), 49.2 (CH), 55.3 (CH_3), 114.4 (CH), 127.1 (CH), 128.9 (CH), 128.9 (CH), 129.2 (CH), 129.8 (CH); HRMS (ESI) calcd for $C_{22}H_{22}ClNO_3S$ $[M + H]^+$ 416.1087, found 416.1095; IR (KBr) 3286, 2932, 2835, 1512, 1322, 1152, 1093, 819 cm^{-1}.

***N*-[2-(4-Chlorophenyl)-2-(2,4,6-trymethoxyphenyl)ethyl]-4-methylbenzenesulfonamide (10):** ^1H NMR (400 MHz, $CDCl_3$) δ 2.42 (s, 3H), 3.61 (s, 6H), 3.64−3.68 (m, 2H), 3.78 (s, 3H), 4.38 (t, J = 6 Hz, 1H), 4.61 (t, J = 8 Hz, 1H), 6.04 (s, 2H), 7.06 (d, J = 8.4 Hz, 2H), 7.13 (d, J = 8.4 Hz, 2H), 7.25 (d, J = 8 Hz, 2H), 7.63 (d, J = 8.4 Hz, 2H); ^{13}C NMR (100 MHz, $CDCl_3$) δ 21.4, 39.1, 45.0, 55.2, 55.4, 91.0, 108.4, 127.0, 128.0, 129.1, 129.4, 131.5, 136.9, 140.4, 142.9, 159.1, 160.4; DEPT-135 NMR δ 21.5 (CH_3), 39.2 (CH), 45.1 (CH_2), 55.3 (CH_3), 55.5 (CH_3), 91.1 (CH), 127.1 (CH), 128.1 (CH), 129.2 (CH), 129.5 (CH); HRMS (ESI) calcd for $C_{24}H_{26}NO_5SCl$ $[M + H]^+$ 476.1298, found 476.1292; IR (KBr) 3257, 2941, 2841, 1608, 1327, 1158, 1092, 814 cm^{-1}.

***N*-[2-(4-Methoxyphenyl)-2-*p*-tolylethyl]-4-methylbenzenesulfonamide (11):** ^1H NMR (400 MHz, $CDCl_3$) δ 2.29 (s, 3H), 2.44 (s, 3H), 3.48 (t, J = 6.8 Hz, 2H), 3.76 (s, 3H), 3.96 (t, J = 8 Hz, 1H), 4.25 (t, J = 6 Hz, 1H), 6.79 (d, J = 7.6 Hz, 2H), 6.94−7.00 (m, 4H), 7.07 (d, J = 7.2 Hz, 2H), 7.30 (d, J = 7.6 Hz, 2H), 7.67 (d, J = 7.6 Hz, 2H); ^{13}C NMR (100 MHz, $CDCl_3$) δ 20.9, 21.5, 47.4, 49.2, 55.2, 114.1, 127.1, 127.6, 128.8, 129.5, 129.5, 132.8, 136.6, 136.7,137.9, 143.4, 158.5; HRMS (ESI) calcd for $C_{23}H_{25}NO_3S$ $[M + H]^+$ 396.1633, found 396.1624; IR (KBr) 3284, 2932, 2813, 1508, 1322, 1153, 1094, 819 cm^{-1}.

4-Methyl-*N*-(2-phenyl-2-thiophen-2-ylethyl)benzenesulfonamide (12): ^1H NMR (400 MHz, $CDCl_3$) δ 2.43 (s, 3H), 3.46−3.60 (m, 2H), 4.28 (t, J = 8 Hz, 1H), 4.40 (s, 1H), 6.78 (s, 1H), 6.92 (s, 1H), 7.13−7.21 (m, 2H), 7.23−7.37 (m, 6H), 7.70 (d, J = 8 Hz, 2H); ^{13}C NMR (100 MHz, $CDCl_3$) δ 21.5, 46.4, 48.4, 124.6, 124.9, 126.3, 127.2, 127.7, 127.8, 128.9, 129.7, 136.7, 140.4, 143.6, 144.2; DEPT-135 NMR δ 21.6 (CH_3), 46.5 (CH), 48.5 (CH_2), 124.7 (CH), 125.0 (CH), 126.4 (CH), 127.3 (CH), 127.8 (CH), 127.9 (CH), 128.9 (CH), 129.8 (CH); HRMS (ESI) calcd for $C_{19}H_{19}NO_2S_2$ $[M + Na]^+$ 380.0755, found 380.0762; IR (KBr) 3292, 2923, 2842, 1598, 1321, 1154, 1092, 816 cm^{-1}.

4-Methyl-*N*-(2-phenyl-2-furan-2-ylethyl)benzenesulfonamide (13): ^1H NMR (400 MHz, $CDCl_3$) δ 2.44 (s, 3H), 3.37−3.44 (m, 1H), 3.55−3.61 (m, 1H), 4.09 (t, J = 7.6 Hz, 1H), 4.44 (s, 1H), 6.01 (d, J = 3.2 Hz, 1H), 6.27 (d, J = 3.2 Hz, 1H), 7.12 (t, J = 8 Hz, 2H), 7.23−7.36 (m, 6H), 7.69 (d, J = 8.4 Hz, 2H); ^{13}C NMR (100 MHz, $CDCl_3$) δ 21.5, 45.1, 46.5, 107.0, 110.2, 127.0, 127.5, 127.9, 128.8, 129.8, 136.8, 138.6, 142.0, 143.5, 154.0; DEPT-135 NMR δ 21.5 (CH_3), 45.2 (CH), 46.6 (CH_2), 107.1 (CH), 110.3 (CH), 127.1 (CH), 127.6 (CH), 128.1 (CH), 128.9 (CH), 129.8 (CH), 142.1 (CH); HRMS (ESI) calcd for $C_{19}H_{19}NO_3S$ $[M + Na]^+$ 364.0983, found 364.0977; IR (KBr) 3448, 1637, 1328, 1160, 1093, 814 cm^{-1}.

4-Methyl-*N*-[2-(5-methylthiophen-2-yl)-2-phenylethyl]benzenesulfonamide (14): ^1H NMR (400 MHz, $CDCl_3$) δ 2.39 (s, 3H), 2.44 (s, 3H), 3.50−3.59 (m, 2H), 4.11 (t, J = 8 Hz, 1H), 4.42 (s, 1H), 6.54 (s, 2H), 7.21 (d, J = 8.8 Hz, 2H), 7.24−7.41 (m, 5H), 7.73 (d, J = 8.4 Hz, 2H); ^{13}C NMR (100 MHz, $CDCl_3$) δ 15.2, 21.5, 46.5, 48.3, 124.8, 127.1, 127.6, 127.8, 128.7, 129.7, 136.7, 139.2, 140.6, 141.8, 143.5; DEPT-135 NMR δ 15.4 (CH_3), 21.6 (CH_3), 46.6 (CH), 48.4 (CH_2), 124.9 (CH), 127.1 (CH), 127.5 (CH), 127.7 (CH), 128.7 (CH), 128.8 (CH), 129.8 (CH); HRMS (ESI) calcd for $C_{20}H_{21}NO_2S_2$ $[M + H]^+$ 372.1092, found 372.1075; IR (KBr) 3291, 2919, 2815, 1598, 1322, 1154, 1093, 816 cm^{-1}.

4-Methyl-*N*-[2-(5-methylfuran-2-yl)-2-phenylethyl]benzenesulfonamide (15): ^1H NMR (400 MHz, $CDCl_3$) δ 2.21 (s, 3H), 2.44 (s, 3H), 3.27−3.41 (m, 1H), 3.46−3.56 (m, 1H), 4.01 (t, J = 8 Hz, 1H), 4.46 (s, 1H), 5.85 (s, 2H), 7.10 (d, J = 8.4 Hz, 2H), 7.16−7.40 (m, 5H), 7.71 (d, J = 8.4 Hz, 2H); ^{13}C NMR (100 MHz, $CDCl_3$) δ 13.8, 21.5, 45.1, 46.6, 106.0, 107.7, 127.0, 127.4, 127.9, 128.8, 129.7, 136.9, 138.9, 143.4, 151.7, 152.0; DEPT-135 NMR δ 13.6 (CH_3), 21.6 (CH_3), 45.2 (CH), 46.7 (CH_2), 106.1 (CH), 107.8 (CH), 127.1 (CH), 127.5 (CH), 128.0 (CH), 128.8 (CH), 129.8 (CH); HRMS (ESI) calcd for $C_{20}H_{21}NO_3S$ $[M + Na]^+$ 378.1140, found 378.1134; IR (KBr) 3298, 2921, 2815, 1598, 1320, 1153, 1093, 816 cm^{-1}.

4-Methyl-*N*-(2-phenyl-2-benzothiophen-2-ylethyl)benzenesulfonamide (16): ^1H NMR (200 MHz, $CDCl_3$) δ 2.43 (s, 3H), 3.54−3.74 (m, 2H), 4.35−4.53 (m, 1H), 7.01−7.53 (m, 10H), 7.65−7.70 (m, 1H), 7.70−7.84 (m, 3H); ^{13}C NMR (54.6 MHz, $CDCl_3$) δ 21.5, 45.1, 47.3, 122.4, 122.8, 124.1, 124.6, 127.1,

127.5, 127.9, 128.1, 128.9, 129.0, 129.8, 135.4, 136.9, 139.6, 140.5, 143.6; LRMS (ESI) $C_{23}H_{21}NO_2S_2$ $[M + Na]^+$ 430.0491.

***N*-[2-(4-Chlorophenyl)-2-furan-2-ylethyl]-4-methylbenzenesulfonamide (17):** ^{1}H NMR δ 2.44 (s, 3H), 3.35−3.42 (m, 1H), 3.51−3.58 (m, 1H), 4.09 (t, J = 7.6 Hz, 1H), 4.43 (t, J = 6.4 Hz, 1H), 6.01 (d, J = 3.2 Hz, 1H), 6.29 (s, 1H), 7.05 (d, J = 8.4 Hz, 2H), 7.23−7.32 (m, 5H), 7.67 (d, J = 8.4 Hz, 2H); ^{13}C NMR (100 MHz, $CDCl_3$) δ 21.5, 44.6, 46.4, 107.2, 110.3, 127.0, 128.9, 129.3, 129.7, 133.3, 136.8, 137.2, 142.2, 143.6, 153.4; DEPT-135 NMR δ 21.6 (CH_3), 44.7 (CH), 46.5 (CH_2), 107.3 (CH), 110.4 (CH), 127.1 (CH), 129.0 (CH), 129.3 (CH), 129.8 (CH), 142.3 (CH); HRMS (ESI) calcd for $C_{19}H_{18}NO_3SCl$ $[M + H]^+$ 376.0774, found 376.0772; IR (KBr) 3288, 2925, 1597, 1322, 1153, 1093, 819 cm^{-1}.

***N*-[2-(4-Chlorophenyl)-2-thiophen-2-ylethyl]-4-methylbenzenesulfonamide (18):** ^{1}H NMR (400 MHz, $CDCl_3$) δ 2.44 (s, 3H), 3.43−3.57 (m, 2H), 4.29 (t, J = 7.6 Hz, 1H), 4.38 (t, J = 6.4 Hz, 1H), 6.77 (d, J = 3.2 Hz, 1H), 6.92 (d, J = 3.6 Hz, 1H), 7.08 (d, J = 8.4 Hz, 2H), 7.18−7.33 (m, 5H), 7.67 (d, J = 8.4 Hz, 2H); ^{13}C NMR (100 MHz, $CDCl_3$) δ 21.5, 45.9, 48.3, 124.8, 125.0, 126.9, 127.0, 128.9, 129.2, 129.8, 133.3, 136.7, 138.9, 139.0, 143.6; HRMS (ESI) calcd for $C_{19}H_{18}ClNO_2S_2$ $[M + H]^+$ 392.0546, found 392.0556; IR (KBr) 3285, 1597, 1321, 1153, 1093, 819 cm^{-1}.

***N*-[2-(4-Chlorophenyl)-2-benzofuran-2-ylethyl]-4-methylbenzenesulfonamide (19):** ^{1}H NMR (400 MHz $CDCl_3$) δ 2.42 (s, 3H), 3.54−3.64 (m, 2H), 4.15−4.17(t, J = 5.2 Hz, 1H), 4.34 (br s, 1H), 6.68−6.72 (d, J = 16 Hz, 1H), 6.91−7. 04 (m, 1H), 7.06−7.12 (m, 2H), 7.15−7.33 (m, 7H), 7.60−7.67 (m, 2H); ^{13}C NMR (100 MHz $CDCl_3$) δ 21.5, 47.4, 50.0, 106.3, 110.6, 121.5, 122.8, 127.0, 128.0, 128.9, 129.1, 129.2, 129.8, 136.6, 139.4, 143.6, 145.0, 145.4, 145.7; HRMS (ESI) calcd for $C_{23}H_{20}ClNO_3S$ $[M + Na]^+$ 448.0750, found 448.0750.

***N*-(2-Furan-2-yl-2-*p*-tolylethyl)-4-methylbenzenesulfonamide (20):** ^{1}H NMR (400 MHz, $CDCl_3$) δ 2.31 (s, 3H), 2.43 (s, 3H), 3.34−3.41 (m, 1H), 3.53−3.60 (m, 1H), 4.04 (t, J = 7.6 Hz, IH), 4.41 (t, J = 6.4 Hz, 1H), 5.98 (s, 1H), 6.27(s, 1H), 6.96 (d, J = 8.4 Hz, 2H), 7.09 (d, J = 8 Hz, 2H), 7.26−7.35 (m, 3H), 7.68 (d, J = 8 Hz, 2H); ^{13}C NMR (100 MHz, $CDCl_3$) δ 20.9, 21.5, 44.7, 46.5, 106.8, 110.2, 127.0, 127.8, 129.5, 129.7, 135.5, 136.9, 137.2, 141.9, 143.4, 154.2; HRMS (ESI) calcd for $C_{20}H_{21}NO_3S$ $[M + H]^+$ 356.1320, found 356.1347; IR (KBr) 3448, 2923, 1638, 1513, 1328, 1160, 1093, 813 cm^{-1}.

***N*-(1,2-Diphenyl-2-thiophen-2-ylethyl)-4-methylbenzenesulfonamide (21):** ^{1}H NMR (400 MHz, $CDCl_3$) δ 2.36 (s, 3H), 4.15 (d, J = 10 Hz, 1H), 4.69 (d, J = 4.8 Hz, 1H), 5.39 (dd, J = 5.2 Hz, J = 4.8 Hz, 1H), 6.48 (d, J = 3.2 Hz, 1H), 6.56 (t, J = 3.6 Hz, 1H), 6.96 (d, J = 4.4 Hz, 1H), 7.02−7.13 (m, 5H), 7.23−7.29 (m, 7H), 7.32 (d, J = 7.6 Hz, 2H); ^{13}C NMR (100 MHz, $CDCl_3$) δ 21.4, 57.0, 59.3, 124.8, 125.8, 126.7, 126.9, 127.1, 127.6, 127.7, 128.24, 128.4, 128.4, 129.0, 137.1, 139.5, 140.2, 142.9, 143.1; HRMS (ESI) calcd for $C_{25}H_{23}NO_2S_2$ [M+Na]$^+$ 456.1068, found 456.1058; IR (KBr) 3449, 1638, 1560, 1325, 1158, 1093, 810 cm^{-1}.

Kinetics Study by Varying Phosphorus Ligands in NMR: Experimental Procedure. In an NMR tube 0.08 mmol of *N*-tosylaziridine **1a** (22 mg) was mixed with 0.0008 mmol of $[Ag(COD)_2]PF_6$ (0.37 mg, which is taken from stock solution of catalyst in $CDCl_3$ solvent) in 400 μL of $CDCl_3$ solvent. Then 0.0016 mmol of PR_3 ligand (for PPh_3 ligand 0.42 mg is required, which is added by preparing stock solution in $CDCl_3$ solvent) was added. Into this mixture then 100 μL of anisole was added. Diphenyl methyl toluene is used as an internal reference (in each kinetic run a fixed amount of 4 mg of the standard was added). The sample was analyzed by ^{1}H NMR spectroscopy. In ^{1}H NMR spectroscopy we monitored the benzylic protons and area under benzylic protons with respect to standard was measured under several time intervals. We have taken 6 points at 20 min intervals, from which the k-values were determined.

Hammett Study with Respect to Aziridine: Experimental Procedure. In an NMR tube 0.08 mmol of para-substituted *N*-tosylaziridine was mixed with 0.0008 mmol of $[Ag(COD)_2]PF_6$ in 400 μL of $CDCl_3$ solvent. Then 100 μL of anisole was added. Here also diphenylmethyltoluene is used as internal standard (for each experiment a fixed amount 4 mg was added). The sample was analyzed by ^{1}H NMR spectroscopy by monitoring the benzylic protons as described before.

ESI-MS Study. Electrospray mass spectra were obtained by using a methanol mobile phase. The solutions of the compounds were prepared as follows:

(i) For silver−phosphine complex: First 5×10^{-3} mmol (2.5 mg) of $[Ag(COD)_2]PF_6$ and 10×10^{-3} mmol (2.62 mg) of PPh_3 were added to 1 mL of methanol (HPLC grade). Then 100 μL of this stock solution was diluted with methanol in 1:10 v/v ratio. The resulting solution was injected directly into the mass spectrometer.

(ii) For silver−trimethoxy benzene complex: (a) Set-1: First 6×10^{-3} mmol (1.5 mg) of $AgPF_6$ and 12×10^{-3} mmol (2 mg) of $C_9H_{12}O_3$ were added to 1 mL of methanol (HPLC grade). Then 100 μL of this stock solution was diluted with methanol in 1:10 v/v ratio. The resulting solution was injected directly into the mass spectrometer. (b) Set-2: First 5×10^{-3} mmol (2.5 mg) of $[Ag(COD)_2]PF_6$ and 10×10^{-3} mmol (1.5 mg) of $C_9H_{12}O_3$ were added to 1 mL of methanol (HPLC grade). Then 100 μL of this stock solution was diluted with methanol in 1:10 v/v ratio. The resulting solution was injected directly into the mass spectrometer.

The solutions of the compounds were injected directly into the spectrometer via a Rheodyne injector equipped with a 10 μL loop. A 20 micro LC syringe pump delivered the solution to the vaporization nozzle of the electrospray ion source at a flow rate of 3 μL min^{-1}. Nitrogen was used both as a drying gas and for nebulization with flow rates of approximately 3 L min^{-1} and 100 mL min^{-1}, respectively.

^{109}Ag NMR Study. The ^{109}Ag spectra were recorded on a 400 MHz spectrometer, using a 5 TBI probe head at a frequency of 18.622 MHz to obtain the signal of the desired intensity; 1 M solution of $AgPF_6$ in $CDCl_3$ was used.

Kinetic Study by Varying Diene Ligands: Experimental Procedure. In an NMR tube 0.08 mmol of *N*-tosylaziridine **1a** (22 mg) was mixed with 0.0008 mmol of $AgPF_6$ (0.20 mg, which was taken from a stock solution of catalyst in $CDCl_3$) in 400 μL of $CDCl_3$. To this solution was added 0.0016 mmol of the respective diene ligand, 100 μL of anisole (to maintain pseudo-first-order condition), and diphenylmethyltoluene as as internal reference (in each kinetic run a fixed amount of 4 mg of the standard was added). The sample was analyzed by ^{1}H NMR spectroscopy by monitoring the benzylic protons as described before.

Acknowledgment. We thank DST (financial support to S.R.), and CSIR (fellowship to M.B.). M.B. especially thanks Shrabani for helpful discussion on the DFT calculation.

Supporting Information Available: Tables, characterization data, kinetic plots, MS, ^{1}H and ^{13}C NMR spectra for all compounds, and crystallographic data for **6**. This material is available free of charge via the Internet at http://pubs.acs.org.